Int. J. Heat Mass Transfer. Vol. 25, No. 9, pp. 1419–1425, 1982
Printed in Great Britain

0017-9310/82/091419-07 $03.00/0
Pergamon Press Ltd.

ORDERED MOTION OF TURBULENCE IN A THERMALLY STRATIFIED FLOW UNDER UNSTABLE CONDITIONS

TOKURO MIZUSHINA, FUMIMARU OGINO and NAOKI KATADA
Department of Chemical Engineering, Kyoto University, Kyoto, Japan

(*Received* 31 *March* 1982)

Abstract—Measurements of the streamwise and vertical velocity fluctuations and temperature fluctuation in a thermally stratified flow in an open channel under unstable conditions were made with two laser Doppler velocimeters and a film probe operated as a resistance thermometer. The result indicates that the contribution to the total turbulent momentum flux from the sweep motion of large amplitude becomes greatest in the free surface region, while that from the ejection motion remains largest in the wall region. The ejection motion makes the largest contribution to the total turbulent heat transport over the whole measurement range from the wall region to the free surface region for both weakly and strongly unstable conditions. The outward interaction motion makes increasing contribution to the total turbulent momentum flux as well as to the total turbulent heat flux and is closely connected with the ejection motion under the strongly unstable conditions. The mean durations and the mean periods of occurrences of the respective motions decrease with increasing instability.

NOMENCLATURE

g, gravitational acceleration [m s^{-2}];
H, threshold;
R, hydraulic radius [m];
Re, Reynolds number, $(4R\langle U\rangle)/\nu$;
$\overline{Ri}$, overall Richardson number, $[\beta g(T_s - T_b)R]/(\langle U\rangle^2)$;
S_i, sorting function;
T, time-averaged temperature [K];
T_b, time-averaged temperature at the bottom wall [K];
T_i, mean period of occurrence of the motion classified into ith quadrant [s];
T_s, time-averaged temperature at the free surface [K];
ΔT_i, mean duration of the motion classified into ith quadrant [s];
t, time [s];
t_0, sampling time [s];
U, time-averaged velocity [m s^{-1}];
U^+, dimensionless time-averaged velocity, U/u_*;
$\langle U\rangle$, cross-sectional mean velocity [m s^{-1}];
u, streamwise velocity fluctuation [m s^{-1}];
u_*, friction velocity [m s^{-1}];
v, vertical velocity fluctuation [m s^{-1}];
y, distance from the wall [m];
y^+, dimensionless distance from the wall, (yu_*/ν).

Greek symbols

δ, flow depth [m];
θ, temperature fluctuation [K];
ν, kinematic viscosity [m^2 s^{-1}];
τ_i, time fraction of the motion classified into ith quadrant [s].

1. INTRODUCTION

THE FLUIDS appearing in environmental heat transfer are usually in motion and often the flow is turbulent. In addition, heat transfer on the environmental scale ordinarily involves a buoyancy effect. It is therefore important to know the interaction between buoyancy and turbulence.

One of the flow configurations important in environmental heat transfer processes with significant buoyancy effects is thermally stratified turbulent shear flow. Important practical cases include the atmospheric boundary layer and flows in rivers or canals involving the disposal of waste water.

The buoyancy effects on the eddy diffusivities of momentum and heat in the thermally stratified flows in an open channel have been investigated [1]. Komori [2] measured the fluctuations of streamwise and vertical velocities and temperature, and discussed the buoyancy effect on their correlations.

In recent years there has been renewed interest in turbulent shear flows. This interest has been generated primarily by visual studies [3, 4] and by some other investigators [5, 6]. These visual studies have revealed that the fluid motions in turbulent flows show a rather definite sequence of ordered motions. The ordered motions have also been investigated by appropriately processed turbulent hot-wire signals or conditional sampling techniques [7–9].

On the other hand, it appears that there has been very little work on the statistical properties of the instantaneous turbulent heat flux $v\theta(t)$. Perry and Hoffmann [10] made measurements of instantaneous turbulent heat fluxes in a turbulent boundary layer flow and divided them into the four quadrants of the v–θ plane. However the physical meaning of such a classification in the v–θ plane is not clear. Interaction

between buoyancy and the ordered motions of turbulence in stably stratified flows has been discussed by Ogino *et al.* [11].

The purpose of the present investigation is to reveal the buoyancy effect on the ordered motions and in turn on the turbulent momentum and heat transfers in a thermally stratified flow under unstable conditions.

2. EXPERIMENT

A complete description of the experimental apparatus has been given [2]. Here we need only describe the main features of the apparatus and the flow relevant to the present measurements.

The experiments were carried out in the 6.1 m flume with a cross section of 0.3 m wide and 0.06 m deep. The side walls and the bottom wall were made of smooth stainless steel plates lined with 0.03 m thickness glass-wool so that the adiabatic conditions were maintained. At the measuring station, 4.2 m downstream from the flume inlet, optical glass plates were installed in the side walls and the bottom floor to enable the use of a laser Doppler velocimeter.

Unstable stratified flow was obtained by providing water heated up to 330–350 K into the flume and by evaporating water from the free surface into the atmosphere. The inlet temperature of the water was controlled within ± 0.05 K in a temperature regulating tank.

Two laser Doppler velocimeters (DISA Type 55X, 55L) were used for the measurement of the streamwise and vertical velocity fluctuations. The temperature fluctuations were measured by a constant current thermometer (DISA 55M20) with a film probe (TSI Model 1264). The voltage outputs from these instruments were directly transmitted to a data acquisition system (TEAC DP-4000) and the signals were digitized and stored on magnetic tape. The sampling frequency was 200 Hz and the sample size about 25 000. Statistical processing of the digitized data was made with the FACOM OS IV/F4 computer system in the Data Processing Center of Kyoto University.

The cross-sectional mean velocities were 0.05–0.09 m s^{-1} and the flow depth was maintained at approx. 0.04 m for each run. Reynolds numbers based on the hydraulic equivalent diameter were 9000–25 000. The overall Richardson number ranged from 0 to -0.151.

3. EXPERIMENTAL RESULTS

3.1. *Time-averaged velocity and temperature profiles*

The distributions of the time-averaged temperature of the unstably stratified flows are shown in Fig. 1. The temperature gradients are large in the region near the free surface where the velocity gradients are usually small, so that the strongly unstable flow can be obtained.

The distributions of the time-averaged velocities are plotted in the form of U^+ against y^+ in Fig. 2. The velocity profile of the isothermal flow is in good agreement with the logarithmic law, while the velocities for unstably stratified flows attains lower values than those for isothermal flow in the region of large temperature gradient due to an increase in the eddy diffusivity of momentum [1].

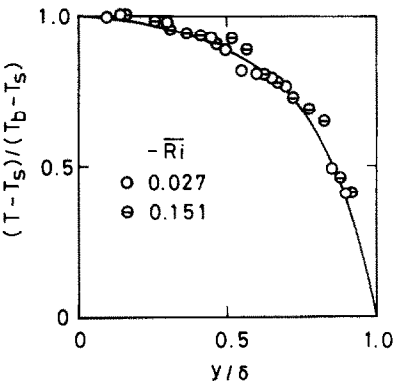

FIG. 1. Distributions of time-averaged temperatures.

3.2. *Contributions to the total Reynolds stress from different turbulent motions*

The statistical and conditional analysis of the instantaneous Reynolds shear stress used in the present investigation is similar to that used by Lu and Willmarth [7].

The signal of the instantaneous Reynolds stress is classified into the four quadrants of the u–v plane and the classified values are then averaged as

$$\widetilde{uv}_i(H) = (1/t_0)\int_0^{t_0} uv(t)S_i(t, H)\mathrm{d}t \qquad (1)$$

where t_0 denotes the sampling time and the subscript i refers to the ith quadrant. The sorting function S_i is defined by

$$S_i(t, H) = 1 \text{ if } |uv(t)| > Hu'v'$$

and the point (u, v) in the u–v plane is in the ith quadrant,

$$0 \text{ otherwise.} \qquad (2)$$

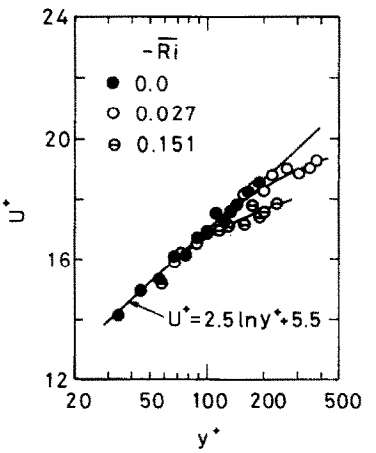

FIG. 2. Distributions of time-averaged velocities.

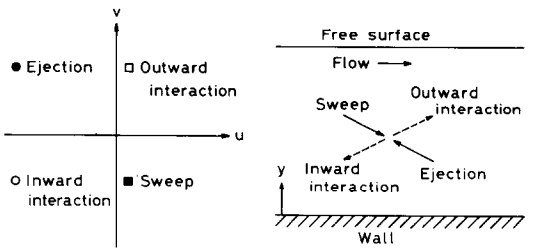

FIG. 3. Sketch of four quadrants of u–v plane and corresponding four turbulent motions.

incoming accelerated fluid is reflected outwards from the wall [12]. The former is called the inward interaction motion and the latter the outward interaction motion. The first and the third quadrants of u–v plane represent respectively the outward and inward interaction motions. The keys depicted in Fig. 3, denoting the four turbulent motions, are used consistently in the subsequent figures in this paper.

The vertical variations of the values of $\widetilde{uv}\,(0)$ normalized with the local average Reynolds stress $\overline{uv}$, are depicted in Figs. 4(a)–(c).

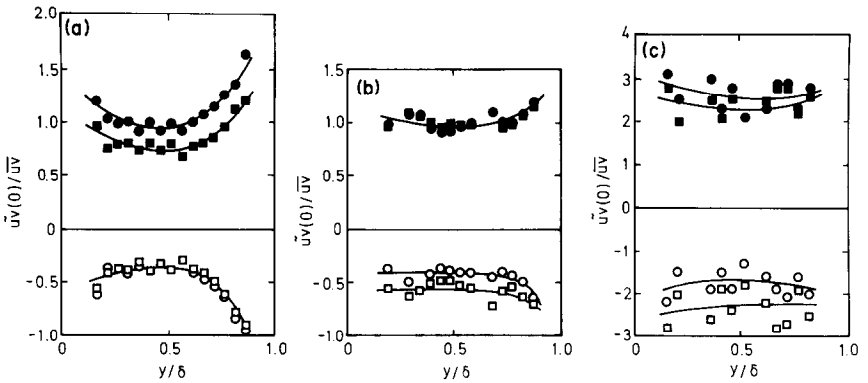

FIG. 4. Contributions to the total Reynolds stress from different turbulent motions with $H = 0$. (a) $\overline{Ri} = 0.0$, (b) $\overline{Ri} = -0.050$, (c) $\overline{Ri} = -0.151$.

where u' and v' are the RMS values of u and v respectively, and large contributors to the total Reynolds stress $\overline{uv}$ from each quadrant can be extracted with the parameter H.

Figure 3 shows the four quadrants of the u–v plane and a schematic drawing of the four turbulent motions corresponding to the four quadrants. The second quadrant in Fig. 3 represents the ejection motion and the fourth quadrant the sweep motion. Between these two larger scale motions there often occurs an interaction in which occasionally the low-speed ejecting fluid is deflected back towards the wall and the

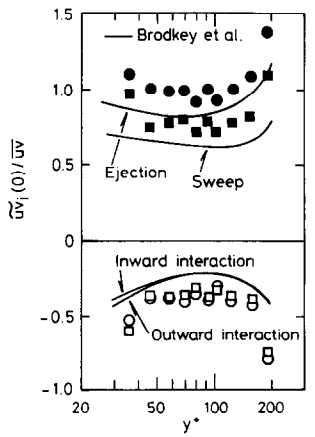

FIG. 5. Variations of $(\widetilde{uv}_i)/(\overline{uv})$ with y^+.

Figure 4(a) shows the measured result of the isothermal flow. The contribution to $\overline{uv}$ from the ejection motion is the largest and those from two interaction motions are the smallest. The present result obtained in the isothermal flow is compared with that obtained in a bounded channel flow [8] in Fig. 5. Although the absolute values of $(\widetilde{uv}_i)/\overline{uv}$ of the present experiment are somewhat greater than those of Brodkey *et al.*, the two sets of the results exhibit similar variations of $(\widetilde{uv}_i)/(\overline{uv})$ with y^+. Thus the importance of the ejection motion is obvious in the isothermal flow in an open channel as well as in the bounded channel flow.

Figures 4(b) and (c) show the results in the unstably stratified flows of $\overline{Ri} = -0.50$ and -0.151 respectively. The result obtained under the weakly unstable condition shows that the contribution of the sweep motion becomes greater and nearly equal to that of the ejection motion over the whole region of $0.2 < (y/\delta) < 0.9$; they are each at about 100% of $\overline{uv}$. The outward interaction motion also makes a greater negative contribution of about 60%, while the contribution of the inward interaction motion remains at about 40%. The result in the strongly unstable flow is depicted in Fig. 4(c), showing the nearly same trend as that in Fig. 4(b). However, all the absolute values of $(\widetilde{uv}_i)/(\overline{uv})$ become very large, that is, the contributions of the ejection and the sweep motions are each nearly equal at about 250% and the negative contributions of

inward and outward interaction motions are roughly 170 and 230% respectively, thus giving the net stress $\overline{uv}$ as required. These large values of $(\widetilde{uv}_i)/(\overline{uv})$ are caused by the fact that the value of $\overline{uv}$ is reduced by the increasing negative contributions of two interaction motions, especially that of outward interaction motion. As shown by Ogino *et al.* [11] the buoyancy effect in the stable stratified flow is to increase the contribution of inward interaction motion, but in the unstable flow the contribution of outward interaction motion seems to be increased by buoyancy effect, both motions contributing to the decrease in the value of $-\overline{uv}$.

As pointed out by Lu and Willmarth [7] and Brodkey *et al.* [8] there does not exist a one-to-one correspondence between the visually observed motions and the four classified motions in the u–v plane. Lu and Willmarth assumed that, if the uv signal reaches or exceeds a certain specified level i.e. the threshold H, in the second quadrant, an ejection or a burst occurs. A similar scheme was used for a sweep. They set H at 4–4.5 for the ejection motion and 2.25–2.75 for the sweep motion. Here we simply set $H = 4$ and analysed the contributions to $\overline{uv}$ from four motions of large amplitude. The results are shown in Fig. 6.

In the isothermal flow only the ejection motion makes a dominant contribution to the Reynolds stress as shown in Fig. 6(a), while in the unstably stratified flows the sweep motion appears to be more important in the free surface region of $(y/\delta) > 4$–5 and the ejection motion remains to be important in the wall region of $(y/\delta) < 4$–5. The shapes of the curves in Fig. 6(c) show a pairing of the ejection motion with the outward interaction motion, suggesting they are closely connected to one mechanism in the strongly unstable flow, though the outward interaction motion is considered to be the reflection of the high velocity sweep motion from the wall in the isothermal flow.

3.3. *Contributions to the total turbulent heat flux from different turbulent motions*

The statistical and conditional analysis of the instantaneous turbulent heat flux $v\theta(t)$ was made in a similar way to that of the instantaneous Reynolds stress.

The signal of the instantaneous turbulent heat flux is classified also into the four quadrants of the u–v plane and the classified values are then averaged as

$$\widetilde{v\theta}_i(H) = \frac{1}{t_0}\int_0^{t_0} v\theta(t)S_i(t, H)\mathrm{d}t. \tag{3}$$

Results with $H = 0$ are shown in Figs. 7(a)–(c). It is seen from Fig. 7 that the contribution to the total turbulent heat flux from the ejection motion appears to be the largest with the sweep motion the second largest. On the other hand, the contributions of two interaction motions become larger with increasing instability and the values of $(\widetilde{v\theta}_1)/(\overline{v\theta})$ and $(\widetilde{v\theta}_3/(\overline{v\theta})$ become equal to those of ejection and sweep motion respectively in the strongly unstable flow. This implies that there exist close connections not only between the ejection and outward interaction motions but also between the sweep and inward interaction motions under the strongly unstable condition.

In general the ejection motion with v positive is considered to transport statistically higher temperature fluid of lower layer of flow, i.e. $\theta > 0$, and the sign of θ in the sweeping fluid with v negative is considered to be negative in the unstable flow. Therefore, one can expect that the heat would be transported upward from the wall by these two larger scale motions and the excess heat transported by these motions would be transported back toward the wall by two interaction motions. However, the experimental results indicate that the sweep motion transports heat toward the wall and the contribution of outward interaction motion is positive.

The reason for this discrepancy is not yet clear, and further study on the turbulent heat transfer without buoyancy effects must be made. The tentative explanation is that the sweeping fluid comes from the upstream region of rather higher temperature than the measuring point and then most of the heat transported by the sweep motion would be transported upward by the ejection motion and the remaining small amount of heat would be transported upward by the outward interaction motion and downward by the inward interaction motion. It should be noted that the con-

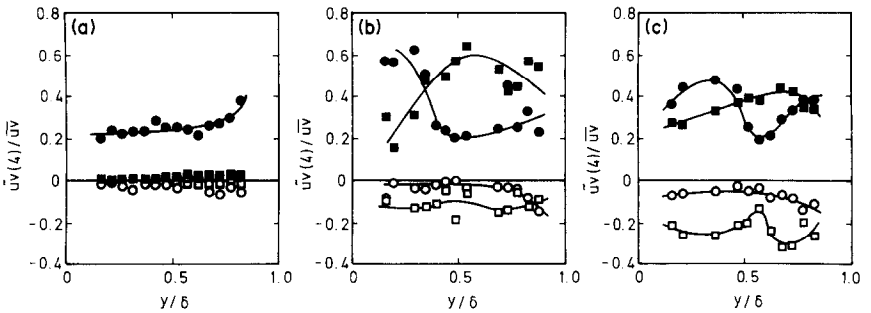

FIG. 6. Contributions to the total Reynolds stress from different turbulent motions with $H = 4$. (a) $\overline{Ri} = 0.0$, (b) $\overline{Ri} = -0.050$, (c) $\overline{Ri} = -0.151$.

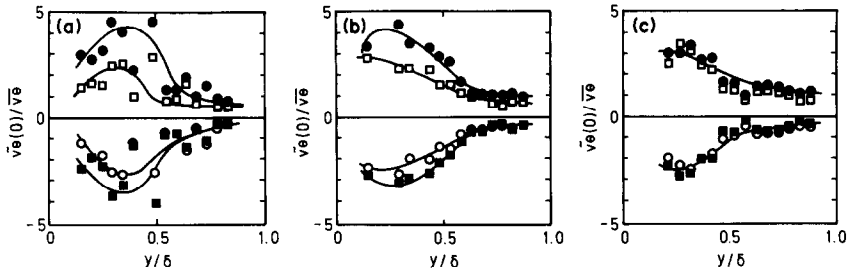

FIG. 7. Contributions to the total turbulent heat flux from different turbulent motions with $H = 0$. (a) $\overline{Ri} = -0.027$, (b) $\overline{Ri} = -0.050$, (c) $\overline{Ri} = -0.151$.

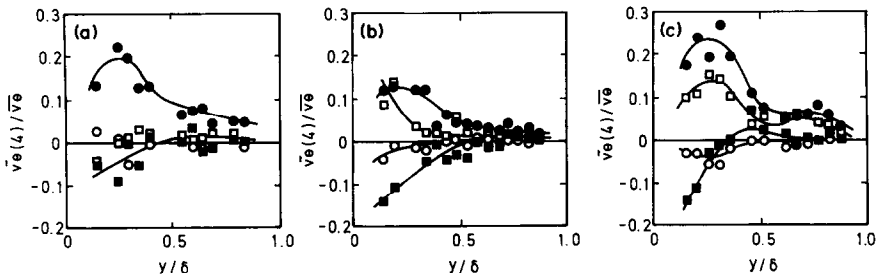

FIG. 8. Contributions to the total turbulent heat flux from different turbulent motions with $H = 4$. (a) $\overline{Ri} = -0.027$, (b) $\overline{Ri} = -0.050$, (c) $\overline{Ri} = -0.151$.

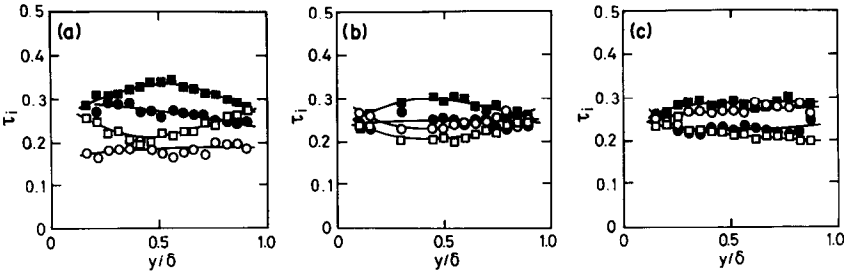

FIG. 9. Time fractions of the respective motions. (a) $\overline{Ri} = 0.0$, (b) $\overline{Ri} = -0.050$, (c) $\overline{Ri} = -0.151$.

dition at the wall is adiabatic in the present experiment.

On the other hand, Fig. 8 indicates that the contribution of the sweep motion of large amplitude with $H = 4$ appears to become positive, although very small, in the free surface region, implying $\theta < 0$ as expected. This may cause the increasing contribution to $\overline{uv}$ from the sweep motion as already shown in Fig. 6.

The contribution of the ejection motion with $H = 4$ is the largest in the wall region except in the vicinity of the wall. The contribution of the sweep motion in the wall region becomes negative and larger with decreasing the distance from the wall to satisfy the adiabatic condition at the wall. Furthermore, the outward interaction motion makes increasing contribution to $\overline{v\theta}$ as well as to $\overline{uv}$, and its curve shape in Fig. 8(c) shows again a pairing with that of the ejection motion at $\overline{Ri} = -0.151$.

3.4. *Time fraction, mean duration and mean period*

The quantity defined by

$$\tau_i = \frac{1}{t_0}\int_0^{t_0} S_i(t, 0)\mathrm{d}t \tag{4}$$

is the fraction of the total time that the signal is in the respective quadrants. The measured results of the fraction of time are shown in Figs. 9(a)–(c). Figure 9(a) shows the result obtained in the isothermal flow and it is seen that the sweep motions occupy about 1/3 of the total time, while the ejection motions roughly 1/4, and two interaction motions each roughly 1/5. Brodkey *et al.* [8] obtained similar results for the bounded channel flow.

Figures 9(b) and (c) show the results obtained in the unstably stratified flows. It is seen that the time fraction of the ejection motion decreases and that of the outward interaction motion increases with increas-

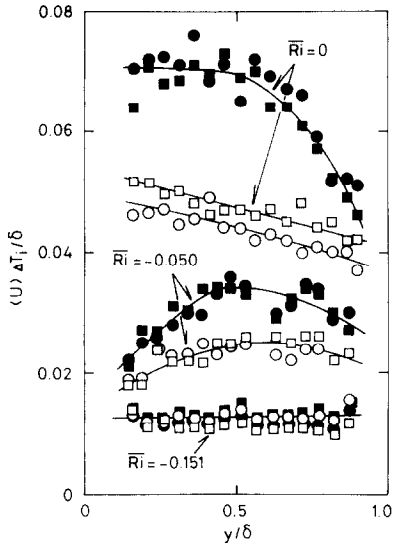

FIG. 10. Mean durations of the respective motions.

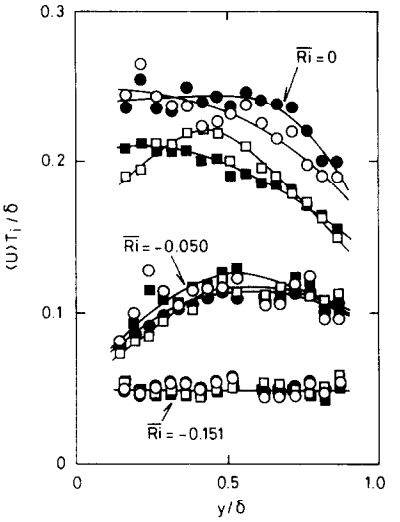

FIG. 11. Mean periods of occurrences of the respective motions.

ing instability, the values of τ_2 and τ_1 becoming nearly equal to those of τ_3 and τ_4 respectively at $\overline{Ri} = -0.151$. This also implies close connections between the ejection and the outward interaction motions and between the sweep and inward interaction motions in the strongly unstable flow.

The mean durations of the respective motions and the mean periods between occurrences of each motion depend on the threshold H. As already noted, Lu and Willmarth set H at 4–4.5 for the measurements of the mean durations and periods of the ejection motions and used a different value of H, 2.25–2.75, for those of the sweep motions. Therefore we simply set $H = 0$ and compare the results in the unstable flows with those in the isothermal flow.

It is seen from Fig. 10 that all the mean durations of four turbulent motions decrease remarkably with increasing instability. If it is assumed that the quantity $(\langle U\rangle\Delta T_i)/\delta$ is a measure of a length scale of the respective motions, the length scales of the ejection and sweep motions appear to be larger than those of two interaction motions in the isothermal flow and the values of them are nearly equal at about 0.07 in the wall region of $(y/\delta) < 0.5$, but decreases with increasing the distance from the wall in the free surface region.

In the weakly unstable flow at $\overline{Ri} = -0.050$ the length scales of these two motions are still larger than those of two interaction motions, but at $\overline{Ri} = -0.151$ all of the length scales of four motions are nearly equal at about 0.013, although the scales of the sweep and the outward interaction motions are seen to be somewhat larger than those of other two motions.

The mean periods of the respective motions are depicted in Fig. 11. The variations of them with increasing instability are similar to those of the mean durations. Thus the buoyancy effect in the unstable flow is to split the respective turbulent motions into smaller scale ones and this results in the decrease of the mean periods, that is, the increase of the occurrence frequency of the respective motions.

4. CONCLUSIONS

The experimental results obtained in the unstably stratified flows are summarized as follows:

(1) The contribution to the total turbulent momentum flux from the sweep motion of large amplitude becomes important in the free surface region, while the contribution from the ejection motion remains largest in the wall region.

(2) The ejection motion makes the largest contribution to the total turbulent heat flux over the whole measurement range from the wall region to the free surface region for both weakly and strongly unstable flows.

(3) The outward interaction motion makes increasing contributions to the total momentum flux as well as to the total heat flux.

(4) There seems to exist close connections between the outward interaction motion and the ejection motion and between the inward interaction motion and the sweep motion.

(5) The mean durations and the mean periods of occurrence of the respective turbulent motions decrease with increasing instability.

Acknowledgement—This work was supported by the Ministry of Education, Science and Culture of Japan through a Grant in Aid for Scientific Research (No. 56116005).

REFERENCES

1. T. Mizushina, F. Ogino, H. Ueda and S. Komori, Buoyancy effect on eddy diffusivities in thermally stratified flow in an open channel, in *Proc. 6th Int. Heat Transfer Conf.* Vol. 1, MC-16, pp. 91–96 (1978).

2. S. Komori, Turbulence structure in stratified flow, Doctoral dissertation, Kyoto University, Kyoto (1980).
3. H. T. Kim, S. J. Kline and W. C. Reynolds, The production of turbulence near a smooth wall in a turbulent boundary layer, *J. Fluid Mech.* **50,** 133–160 (1971).
4. E. R. Corino and R. S. Brodkey, A visual investigation of the wall region in turbulent flow, *J. Fluid Mech.* **37,** 1–30 (1969).
5. S. J. Kline, W. C. Reynolds, F. A. Schraub and P. W. Runstadler, The structure of turbulent boundary layers, *J. Fluid Mech.* **30,** 741–773 (1967).
6. A. J. Grass, Structural features of turbulent flow over smooth and rough boundaries, *J. Fluid Mech.* **50,** 233–255 (1971).
7. S. S. Lu and W. W. Willmarth, Measurements of the structure of the Reynolds stress in a turbulent boundary layer, *J. Fluid Mech.* **60,** 481–511 (1973).
8. R. S. Brodkey, J. M. Wallace and H. Eckelmann, Some properties of truncated turbulence signals in bounded shear flows, *J. Fluid Mech.* **63,** 209–224 (1974).
9. J. Sabot and G. Comte-bellot, Intermittency of coherent structures in the core region of fully developed turbulent pipe flow, *J. Fluid Mech.* **74,** 767–796 (1976).
10. A. E. Perry and P. H. Hoffmann, An experimental study of turbulent convective heat transfer from a flat plate, *J. Fluid Mech.* **77,** 355–368 (1976).
11. F. Ogino, Y. Tominari and T. Mizushina, Heat transfer mechanism in a thermally stratified turbulent flow, to be published in *Proc. 7th Int. Heat Transfer Conf.* (1982).
12. J. M. Wallace, H. Eckelmann and R. S. Brodkey, The wall region in turbulent shear flow, *J. Fluid Mech.* **54,** 39–48 (1972).

MOUVEMENT ORDONNE DE LA TURBULENCE DANS UN ECOULEMENT THERMIQUEMENT STRATIFIE SOUS UNE CONDITION INSTABLE

Résumé—Des mesures de fluctuation de vitesse et de température dans un écoulement thermiquement stratifié dans un canal ouvert sous une condition instable sont faites avec deux vélocimètres laser Doppler et une sonde à film chaud. Les résultats montrent que la contribution au flux turbulent total de la quantité de mouvement depuis le mouvement de balayage, de large amplitude, devient la plus grande dans la région de la surface libre, tandis que celle depuis le mouvement d'éjection devient la plus forte dans la région pariétale. Le mouvement d'éjection donne la plus grande contribution au transport total turbulent de chaleur dans tout le domaine de mesure depuis la région pariétale jusqu'à la surface libre, à la fois pour les conditions instables faibles et fortes. Le mouvement d'intéraction accroît la contribution du flux total turbulent de quantité de mouvement aussi bien que du flux thermique total et il est étroitement lié au mouvement d'éjection pour la condition fortement instable. Les durées moyennes et les périodes moyennes d'occurrence des mouvements respectifs décroissent quand l'instabilité augmente.

GEORDNETE TURBULENZBEWEGUNG IN EINER THERMISCH GESCHICHTETEN STRÖMUNG UNTER INSTABILEN BEDINGUNGEN

Zusammenfassung—Mit zwei Laser-Doppler-Anemometern und einer Filmsonde, die als Widerstandsthermometer arbeitete, wurden Messungen der strömungsparallelen und vertikalen Geschwindigkeits- und Temperaturschwankungen in einem offenen Kanal unter instabilen Bedingungen durchgeführt. Das Ergebnis zeigt, daß der Beitrag der Austauschbewegung mit größer Amplitude zum gesamten turbulenten Impulsstrom an der freien Oberfläche am größten wird, während der Beitrag der vom turbulenten Bersten herrührenden Bewegung in Wandnähe am größten bleibt. Die Berstbewegung liefert über den gesamten Meßbereich, vom Wandbereich bis zur freien Oberfläche, sowohl für schwach als auch für stark instabile Bedingungen den größten Beitrag zum gesamten turbulenten Wärmetransport. Die äußere Wechselwirkungsbewegung liefert einen zunehmenden Beitrag zum gesamten turbulenten Impulsstrom sowie zum gesamten turbulenten Wärmestrom und ist eng mit der Berstbewegung unter stark instabilen Bedingungen verknüpft. Die mittere Dauer und die mittlere Periode für das Auftreten der entsprechenden Bewegungen sinken mit zunehmender Instabilität.

УПОРЯДОЧЕННАЯ СТРУКТУРА ТУРБУЛЕНТНОСТИ В ТЕРМИЧЕСКИ НЕУСТОЙЧИВО СТРАТИФИЦИРОВАННОМ ПОТОКЕ

Аннотация—Выполнены измерения продольных и поперечных пульсаций скорости и температуры при термически неустойчиво стратифицированном течении в открытом канале с помощью двух лазерных допплеровских анемометров и пленочного датчика, работающего как термометр сопротивления. Результаты показывают, что наибольший вклад в суммарный перенос импульса около свободной поверхности вносят крупномасштабные возмущения типа обрушивающихся волн, а в области стенки–возмущения типа выбросов. Выбросы дают наибольший вклад в суммарный турбулентный перенос тепла во всем объеме–от области стенки до свободной поверхности–как при слабой, так и сильной неустойчивости. Процесс взаимодействия движения жидкости в области свободной поверхности с внешней средой, оказывающий большое влияние на суммарный турбулентный перенос импульса, а также суммарный турбулентный перенос тепла, тесно связан с появлением выбросов при сильно неустойчивых условиях. Средняя продолжительность и средняя чередуемость выбросов уменьшаются с увеличением неустойчивости.